Exploratory Tactile Servoing With Active Touch

Nathan F. Lepora, *Member, IEEE*, Kirsty Aquilina, and Luke Cramphorn, *Student Member, IEEE*

***Abstract*—A key unsolved problem in tactile robotics is how to combine tactile perception and control to interact robustly and intelligently with the surroundings. Here, we focus on a prototypical task of tactile exploration over surface features such as edges or ridges, which is a principal exploratory procedure of humans to recognize object shape. Our methods were adapted from an approach for biomimetic active touch that perceives stimulus location and identity while controlling location to aid perception. With minor modification to the control policy, to rotate the sensor to maintain a relative orientation and move tangentially (tactile servoing), the method applies also to tactile exploration. Robust exploratory tactile servoing is then attained over various two-dimensional objects, ranging from the edge of a circular disk, a volute laminar, and circular or spiral ridges. Conceptually, the approach brings together active perception and haptic exploration as instantiations of a common active touch algorithm, and has potential to generalize to more complex tasks requiring the flexibility and robustness of human touch.**

***Index Terms*—Force and tactile sensing, biomimetics.**

I. Introduction

TACTILE sensing is widely recognized as necessary for future robots to physically interact with their surroundings in a controlled and robust way, enabling progress in applications such as autonomous manufacturing and personal assisted living. Yet the combination of robust control with tactile sensing and perception is proving elusive. Over the last few years there have been several physical demonstrations of combined tactile control and perception, e.g. [1]–[5]. However, progress is still far from a general purpose solution with the flexibility and robustness of human touch.

A principal issue for robot touch is that tactile sensation depends upon how a tactile sensor contacts a stimulus. Therefore, the coupling between motion and sensing must be a principal aspect of artifical tactile perception [6], [7], as supported by numerous human and animal studies on active touch. Recent work on biomimetic active touch with fingertips and whiskers [8] spans robotics and neuroscience by combining an evidence accumulation model of perceptual decision making with a control policy for overt focal attention to regulate how the tactile sensor contacts a stimulus. In consequence, the tactile perception attains superesolved accuracy (hyperacuity) [9], [10] and is robust to uncertainty in sensor placement [11].

Fig. 1. Tactile robotic system, comprising a tactile fingertip (the TacTip) mounted as end effector on a 6-DOF robot arm.

The aim of this letter is to examine how biomimetic active touch [8] applies to exploring surface features (e.g. edges). Tactile exploration represents a prototypical task that combines tactile sensing and control, and is of psychophysical importance in humans as a basic exploratory procedure for recognizing objects [12]. Earlier work had an inner active perception loop within an exploration control loop [2], [3], [13]. Here we consider instead a single control loop for both active perception and exploration. The tactile sensor explores around an object by maintaining its perceived orientation relative to surface feature or edge and moving tangentially (termed servoing) while tuning its normal displacement to ensure robust perception (termed active perception). A supplementary video clip shows this task being performed.

The performance is validated on several exploratory tasks with a biomimetic tactile fingertip (Fig. 1), including edge following around circular disks and volute (spiral) laminae of varying curvature. Further generality is demonstrated by tracing curved ridges, rather than edges. Robust exploration does require some tuning of the gains for controlling the sensor, but

Manuscript received September 16, 2016; accepted January 11, 2017. Date of publication January 31, 2017; date of current version March 1, 2017. This letter was recommended for publication by Associate Editor J. McInroy and Editor J. Wen upon evaluation of the reviewers' comments. The work of N. F. Lepora was supported in part by the Grant from the Engineering and Physical Sciences Research Council (EPSRC) on "Tactile Superresolution Sensing" (EP/M02993X/1). The work of K. Aquilina and L. Cramphorn was supported by the EPSRC CDT studentships.

The authors are with the Department of Engineering Mathematics and Bristol Robotics Laboratory, University of Bristol, Bristol BS8 1TH, U.K. (e-mail: n.lepora@bristol.ac.uk; ka14187@bristol.ac.uk; ll14468@bristol.ac.uk).

This letter has supplementary downloadable material available at http://ieeexplore.ieee.org, provided by the authors. The Supplemental Material contains a video showing an example of exploratory tactile servoing being performed. This material is 9 MB in size.

Color versions of one or more of the figures in this letter are available online at http://ieeexplore.ieee.org.

Digital Object Identifier 10.1109/LRA.2017.2662071

we found a standard set of values that generally give good performance. Overall the approach works robustly and straightforwardly on all considered tasks, and holds promise to generalize to more complex tasks in higher dimensions with more sophisticated control.

II. Background and Related Work

The focus of this letter is around using active tactile perception to control a robot. In general, active touch combines a method for controlling a sensor with interpretation of that data, using control based on the interpreted data, and has been considered both in human psychophysics [14] and robot control [6], [7], [15]. An influential definition of active perception was made by Bajcsy as 'purposefully changing the sensor's state parameters according to sensing strategies' such that these controlling strategies are 'applied to the data acquisition process which will depend on the current state of the data interpretation and the goal or the task of the process' [15].

For a task, we consider tactile exploration, where the goal is for a tactile sensor to explore the unknown perimeter or an extended feature (e.g. a ridge or edge) around an object. Robotics work on tactile edge following dates back a quarter of a century [16], [17], and has focussed on edge following with image processing techniques such as median filters, Hu transforms and, more recently, geometric moments [18] and image dilation [19]. Image processing techniques have also been integrated into a control framework for tactile servoing to follow extended features such as planar wires [4].

Over the last few years, multiple approaches have been proposed that combine tactile sensor control with perception. When the control of the sensor is the main goal, then the work has has been termed tactile servoing [4], exploration [20] or manipulation [1], [5], [21]. When the perception is the main goal, this work has been termed active perception [11] or active exploration [22]. Here we use a method for biomimetic active perception that decides upon an object's location and identity (e.g. edge position and angle on the sensor) over multiple contacts while actively controlling that location based on the object perception [8].

This work builds on past studies of using active perception to control an iCub fingertip mounted on a 2D Cartesian robot to follow an edge [2], [3], [13], where the active perception loop was instead embedded in another exploration loop with the sensor orientation held fixed – i.e. there was no tactile servoing. In the present letter, we show that exploratory tactile servoing results in a greatly reduced training phase (1/4 the number of angle classes), applies to a wider range of objects (including both edges and ridges), links to recent progress on biomimetic active touch [8] and brings in aspects of control that hold promise to extend to more complex tasks.

III. Methods

A. Robotic System: Tactile Sensor Mounted on a Robot Arm

1) The Tactile Fingertip (TacTip): In this study, we use a tactile sensor developed our lab – the BRL TacTip. Originally developed in 2009 [23], it has since progressed through many design improvements to result in the present version, TacTip v2 (Fig. 2, left). This tactile sensor has a 40 mm-diameter hemispherical sensing pad with 127 tactile pins arranged in a triangular hexagonal lattice with pin-to-pin spacing $\sim$3 mm (Fig. 2, right). Deformation of the sensing pad is transduced into pin movements, with the pin displacements tracked optically in 2D using a webcam CCD and circuit board (resolution 640 $\times$ 480 pixels, sampled at $\sim$20 fps) mounted inside the central column. Image capture and preprocessing uses opencv (http://opencv.org/); pin detection and localization uses a Gaussian spatial filter with adaptive threshold; and pin tracking uses a nearest neighbour algorithm. Similar methods are used in other recent letters [10], [24], [25].

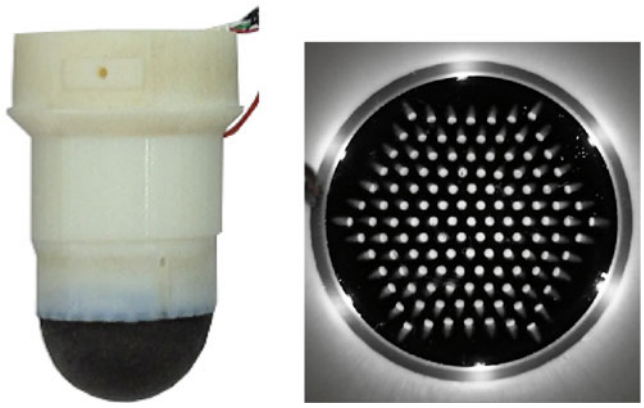

Fig. 2. The tactile fingertip (TacTip) - a 3D-printed modular optical tactile sensor (left) comprising a compliant tip containing the sensing elements, main housing for the electronics and CCD camera, and a standalone base. Right: image from internal CCD showing the array of sensing elements.

The performance of the TacTip compares well with state-of-the-art tactile sensors such as the iCub skin and fingertips, as demonstrated in a recent comparative study of sensor performance in biomimetic active touch [8]. Moreover, the TacTip design lends itself to tactile superresolution [9], giving a localization accuracy ~ 0.1mm that is $30\times$ finer than the sensor resolution given by the pin spacing [10].

2) Robot Arm Mounting: The TacTip is mounted as an end-effector on a six degree-of-freedom robot arm (IRB 120, ABB Robotics) that can precisely and repeatedly position the sensor (absolute repeatability 0.01 mm). The removable base of the TacTip is bolted onto a mounting plate attached to the rotating (wrist) section of the arm, then the other two modular components (central column and tip) are attached by bayonet fittings, resulting in a rigid yet easily detachable assembly. The USB cable from the TacTip is attached by a cable tie to the arm, with enough slack that rotating the end-effector does not pull the cable out of the base (Fig. 1).

3) Integrated Sensing and Control: A modular software framework is deployed whereby the main control and perception algorithms are implemented in MATLAB on a standard windows 2007 PC, which communicates via TCP/IP ports with software that (i) sends control commands to the robot arm; and (ii) receives and pre-processes the TacTip data. The robot arm has its own controller running a native RAPID API (in C#), to which we interface an iron python client on the PC that converts MATLAB outputs into local variables for custom RAPID

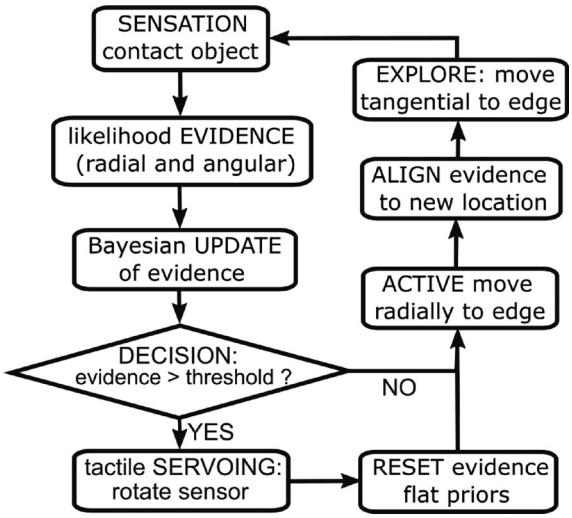

Fig. 3. Biomimetic active touch applied to exploratory tactile servoing. During each perceptual decision, sensory data from discrete tactile contacts is fed into a likelihood model for radial displacement and edge angle, which updates evidence represented as posteriors that is used to move the sensor radially to maintain contact with the edge and explore by moving tangentially along the edge. After a perceptual decision when the evidence crosses a threshold, the sensor is rotated to maintain relative alignment with the edge (termed servoing) and the posteriors reset to start a new decision.

routines to reposition the arm. Simultaneously, a python server on the PC receives data via USB from the TacTip, implements the opencv pre-processing described above, and outputs a multi-dimensional time series of tactile sensor values to MATLAB. The system is capable of real-time operation with sub-second latency, although in practise the ABB arm is capable only of point-to-point position control and so the tactile data is processed in $\sim$1 sec segments. Hence, for simplicity, the MATLAB code is implemented as a state machine, with each segment of tactile data received and processed to determine the control commands to send to the arm, cycling about once per second.

B. Algorithmic Methods: Biomimetic Active Perception

Our method for tactile perception and control has been developed over a series of publications [9], [11], [26] and recently consolidated in a synthetic treatment of biomimetic active touch for a range of tactile sensors [8]. In this work, we follow the conceptualization and notation from that recent study [8] adapted to the present task of tactile exploration.

Biomimetic active touch is defined by three principles based on biological perception (Fig 3): (i) an underlying decision making part based on leading models from perceptual neuroscience; (ii) an action selection part enacted during the decision making, which includes active movement strategies based on human and animal focal attention; and (iii) sensory encoding of how percepts relate to stimuli, here considered as a probabilistic model with analogues to neural coding.

We now describe how these three principles apply to tactile exploration. Further details such as their biological basis can be found in the original reference [8].

1) Perceptual Decision Making: The first component of biomimetic tactile perception is to implement a perceptual decision process in which evidence for distinct perceptual classes is summed until reaching a threshold that triggers the decision, with competition between the alternatives. Mathematically, this evidence accumulation process can be represented by recursive Bayesian analysis (e.g. [8]).

Here we implement evidence accumulation to threshold for a tactile sensor making successive contacts z_t ($t = 1, 2, ...$) with a stimulus. Every contact gives an increment of evidence for each perceptual class according to the likelihoods of that contact $P(z_t|r_l, \theta_i)$, taken over the normal radial displacement from the edge r_l and edge orientation θ_i (discretized into N_r and N_θ classes, respectively). Evidence accumulation is implemented with Bayes' rule applied recursively, represented by the posterior belief

$$P(r_l, \theta_i|z_{1:t}) = \frac{P(z_t|r_l, \theta_i)P(r_l, \theta_i|z_{1:t-1})}{P(z_t|z_{1:t-1})}, \qquad (1)$$

with competition between alternatives from the normalization

$$P(z_t|z_{1:t-1}) = \sum_{l=1}^{N_r}\sum_{i=1}^{N_\theta} P(z_t|r_l, \theta_i)P(r_l, \theta_i|z_{1:t-1}), \qquad (2)$$

according to the marginal probability of the current contact given the previous contact.

The perception is complete when a marginal belief for edge orientation reaches a decision threshold $p_{\rm dec}$, when the *maximal a posteriori* estimate of the angular class is taken:

$$\text{if any} \quad P(\theta_i|z_{1:t_{\rm dec}}) = \sum_{l=1}^{N_r} P(r_l, \theta_i|z_{1:t_{\rm dec}}) > p_{\rm dec}$$
$$\text{then} \quad \theta_{\rm dec} = \arg\max_{\theta_i} P(\theta_i|z_{1:t_{\rm dec}}). \qquad (3)$$

The decision threshold is free parameter that trades off the number of contacts $t_{\rm dec}$ to make a decision against decision accuracy (here set at $p_{\rm dec} = 2/N_\theta$ to give $t_{\rm dec} \lesssim 3$).

During the perceptual decision, an intermediate estimate of the normal displacement will be used for active perception

$$r_{\rm est}(t) = \arg\max_{r_l} \sum_{i=1}^{N_\theta} P(r_l, \theta_i|z_{1:t}), \qquad (4)$$

as described below in Section III-B2 on action selection.

For a task such as tactile exploration, the perceptual decisions are made consecutively with the result of each decision used to control the robot. Therefore the decision making parts of the algorithm for biomimetic active perception (Fig. 3) are complemented with a reset stage that sets $t = 0$ and flat priors $P(r_l, \theta_i|z_0) = 1/N_r N_\theta$. In principle, evidence from previous decisions could contribute [2], but for simplicity we consider here only flat (uniform) prior evidence.

2) Action Selection: The second component of biomimetic active perception is the selection between alternative actions during perception (*i.e.* deciding 'where to move next'). These actions are selected with a control policy that inputs the perceived angle class and intermediate estimates of the radial displacement class. The policy makes an action that combines rotating the sensor towards the currently perceived edge angle after an angle decision, with a tangential (exploratory) move along the

edge and a normal (active perception) move onto the edge after every contact.

The tactile servoing part of the action orients the sensor towards the perceived edge angle $\theta_{\rm dec}$ by trying to maintain a fixed angle $\theta_{\rm fix}$ relative to the edge

$$\Delta\theta = \pi_\theta \left[P(r_l, \theta_n | z_{1:t_{\rm dec}})\right] = \left[\, g_\theta(\theta_{\rm fix} - \theta_{\rm dec}) \,\right]_i , \qquad (5)$$

and performed immediately after a decision. Here the fixation is chosen in the center of the perceptual range $\theta_{\rm fix} = 0^\circ$. The notation $[\cdot]_i$ represents that the action is rounded down to the nearest edge angle class θ_i, including an angular gain g_θ factor (here 0.5 or 1).

The exploratory part of the action moves the sensor tangentially along the edge by a fixed amount Δe (here set to 3 mm), and is performed after every contact (in combination with the corrective component of the action below). The direction of movement is always given by the $\theta = 0^\circ$ egocentric angle class relative to the sensor orientation; in practise, the center of the angular range is kept as an allocentric variable that is initialized at 0° and is updated by $\Delta\theta$ after every angle action.

The corrective component of the action moves the sensor radially towards a pre-set fixation radial displacement $r_{\rm fix}$ relative to the edge. The direction of movement is perpendicular $\theta = 90^\circ$ relative to the sensor orientation, and its magnitude proportional to the distance from the currently estimated normal displacement class

$$\Delta r(t) = \pi_r \left[P(r_l, \theta_n | z_{1:t})\right] = \left[\, g_r(r_{\rm fix} - r_{\rm est}(t)) \,\right]_l , \qquad (6)$$

and performed after every contact. Here the fixation displacement is chosen in the center of the perceptual range $r_{\rm fix} = 0$ mm, which is aligned to center on the edge. The notation $[\cdot]_l$ represents rounding down to the nearest normal radius class r_l, including the gain factor g_r (here 0.5 or 1).

Following previous work on biomimetic active touch [8], [11], after every action for active perception (radially along the normal) it is necessary to make a compensatory transformation of the perceptual beliefs to maintain an allocentric frame for the beliefs

$$P(r_l, \theta_i | z_{1:t}) \leftarrow P([r - \Delta r(t)]_l, \theta_i | z_{1:t}). \qquad (7)$$

For simplicity, the (undetermined) beliefs shifted from outside the location range are assumed uniformly distributed.

3) Sensory Encoding: The third component of biomimetic active perception encodes the sensory data as evidence to be used in the perceptual decision making and action selection. A standard 'histogram' likelihood model has been used in our work on robot touch, originally defined in relation to sensory processing [26], which we summarise here and refer to [8] for further details.

Here we consider data z_t that is a multi-dimensional time series of sensor values,

$$z_t = \{s_k(j) \,:\, 1 \le j \le N_{\rm samples},\ 1 \le k \le N_{\rm dims}\}, \qquad (8)$$

with index j denoting the time sample and k the sensor dimension (x- and y-components of pin movement).

The sensory encoding determines the increment of evidence for each perceptual class, based on the logarithm of a likelihood model of the contact data from training

$$\log P(z_t | r_l, \theta_i) = \sum_{j=1}^{N_{\rm samples}} \sum_{k=1}^{N_{\rm dims}} \frac{\log P_k(s_k(j) | r_l, \theta_i)}{N_{\rm samples} N_{\rm dims}} \qquad (9)$$

assuming statistical independence between all data dimensions k and time samples j. A histogram method is then applied to the training data to give $P_k(s_k | r_l, \theta_i) = P_k(b | r_l, \theta_i)$, binning the sensor values s_k into $N_{\rm bins} = 100$ intervals [8].

C. Task: Exploratory Tactile Servoing

Here we consider tasks in which a tactile sensor moves along a continuously extended tactile feature, such as the edge of an object or ridge across a surface, while maintaining alignment with that feature using biomimetic active perception. We consider this to be an exploration task because the sensor moves onto a previously unknown part of the object and tactile servoing because the sensor moves to maintain its angle of alignment with the stimulus feature (here the edge).

For simplicity, we consider planar objects with the axis of the tactile sensor perpendicular to that plane. We also assume that the sensor can be moved along the plane to maintain a constant depth with each contact. In practise, there will be small deviations from these conditions that affect the tactile sensing, and part of the challenge of this task is to be robust to this form of 'noise'.

Here we consider 'tapping' contacts, where the tactile sensor begins a sensing movement away from the surface (here $\sim$2 mm), taps vertically down onto the surface by a fixed distance (here 5 mm), and then returns back to its original position. This tapping motion is supposed to have a fixed duration (here about 15 time samples over $\sim$1 sec), although again there will be variations due to issues such as network delays (between the PC and robot) and deviations in camera frame rate, which are also treated as 'noise'. Our use of tap-based sensing conveniently segments data for the state machine and reduces sensor hysteresis that would otherwise introduce significant history dependence into the sensing.

The task has a training phase, in which the sensory encoding model (Section III-B3) is learned off-line, and a distinct testing phase, in which the tactile servoing is implemented in real-time on the tactile robotic system.

1) Training: For training, the tactile robotic system samples a local region (e.g. an edge) of a planar object over a range of normal radial displacements and angles (Fig. 4, right diagram). In the terminology of our methods for biomimetic active touch (Section III-B2), the sensor systematically samples a grid of N_r 'where' r_l radial displacements normal to an edge, and N_θ edge angles θ_i by rotating the sensor about its axis. Here we consider $N_r = 20$ locations spanning $-9 \le r_l \le 10$ mm centred (approximately) on an edge, and $N_\theta = 9$ angles spanning $-40^\circ \le \theta_i \le 40^\circ$. Examples from the training data show the sensor readings over the location range for one angle $\theta = 0^\circ$ (Fig. 4(A), (B)) and over the angle range for a central location at $r = 0$ mm (Fig. 4(C) and (D)).

2) Testing: For testing, the tactile robotic system seeks to move around the perimeter of a planar object by perceiving

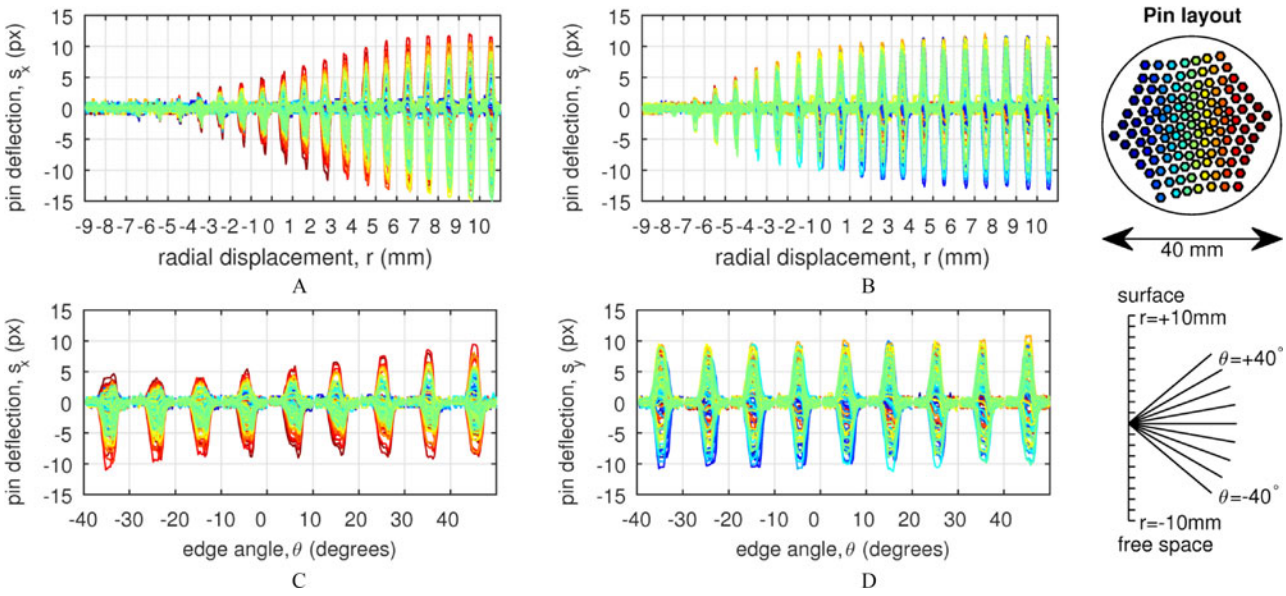

Fig. 4. Tactile data for the TacTip contacting an edge of a circular disk. Contacts were at a constant rate of one tap every second with 1 mm displacement normal to the edge after every tap to span a 20 mm location range (panels A and B); this is repeated for 9 rotations of the sensor between $-40°$ and $+40°$ in $10°$ steps (panels C and D). The color of the plotted trace corresponds to the pin locations (color scheme to top right) and its magnitude the x-deflection (panels A,C) or y-deflection (panels B,D) of the pin from its initial position at the beginning of the contact. (A) Tac Tip x-data for edge angle $\theta = 0$ degrees. (B) Tac Tip y-data for edge angle $\theta = 0$ degrees. (C) Tac Tip x-data for radial displacement $r = 0$ mm. (D) Tac Tip y-data for radial displacement $r = 0$ mm.

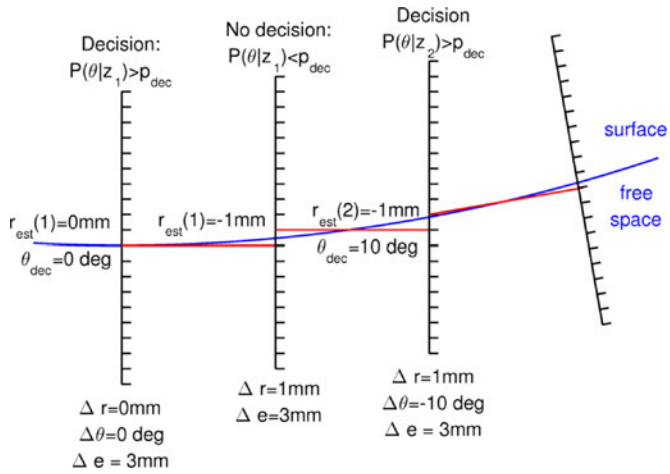

Fig. 5. Exploratory tactile servoing, shown over a few steps of the control loop from Fig. 3 (with unit radial and angular gains in this example). After each contact, the sensor makes an exploratory move Δe tangential to the edge, and a radial move Δr towards the fixation point $r_{\rm fix} = 0$ mm based on the estimated radius $r_{\rm est}$. An angle decision $\theta_{\rm dec}$ is made when the angle posterior crosses a threshold, defining a rotation $\Delta\theta$ towards the fixation angle $\theta_{\rm fix} = 0°$ relative to the edge. Hence the control tries to maintain the same sensor orientation and displacement with respect to the edge, with the radial and tangential directions of motion rotating with the sensor.

the edge angle and radial location relative to the sensor, which define three movements (Fig. 5): (i) active perception moves Δr along the (estimated) normal to the edge to relocate the sensor towards a fixation point $r_{\rm fix}$ relative to the estimated location $r_{\rm est}$; (ii) exploratory moves Δe along the (estimated) tangent to the edge with perceived angle $\theta_{\rm dec}$; and (iii) reorientation of the sensor $\Delta\theta$ towards an angle fixation $\theta_{\rm fix}$ relative to the edge. Here we use a location training range symmetric about the edge, and hence take a central fixation point $r_{\rm fix} = 0$ mm. Similarly, the angle fixation is also at the central point $\theta_{\rm fix} = 0°$. During testing, the robot begins at the fixation points and seeks to maintain them over the task.

The perception and control algorithm proceeds sequentially (Figs. 3 and 5), with an active perception loop for individual radial displacement and edge angle perceptual decisions, interleaved with initialization steps that reset the evidence and re-orient the tactile sensor towards the perceived edge orientation. Individual perceptual decisions are made according to an evidence accumulation process (Section III-B1) up to a preset decision threshold that balances the accuracy of a decision against the number of taps needed to achieve that accuracy. Here we manually set the threshold at $E_{\rm dec} = \log 2/N_\theta = \log 2/9$ to decide typically over 1–3 contacts.

IV. Results

A. Perception of Edge Location and Angle

For an initial validation, we first check that the biomimetic perception methods (Section III-B) can accurately perceive edge angle and radial displacement. We consider a basic validation with the threshold set to give a decision after only one contact $E_{\rm dec} = \log 1/N_{\rm id} = \log 1/9$. We also check that a location range centred on the edge is appropriate, with fixation point in the center of the range.

The data collection was ran twice, to give a first set for training and a second for offline validation (shown in Fig. 4). To assess the edge angle error, we apply the Bayesian perception method (Section III-B) to the perceived radial location and edge angle $(r_{\rm dec}, \theta_{\rm dec})$ and compare with the ground truth (r, θ). Errors are averaged over multiple test runs, with angle error $e_\theta(r,\theta) = \langle|\theta_{\rm dec} - \theta|\rangle$ over runs with the same ground truth (r, θ), and mean angle error $\bar{e}_\theta(r) = \sum_{i=1}^{N_\theta} e_\theta(r, \theta_i)/N_\theta$. Averages were taken over 10,000 randomly generated runs.

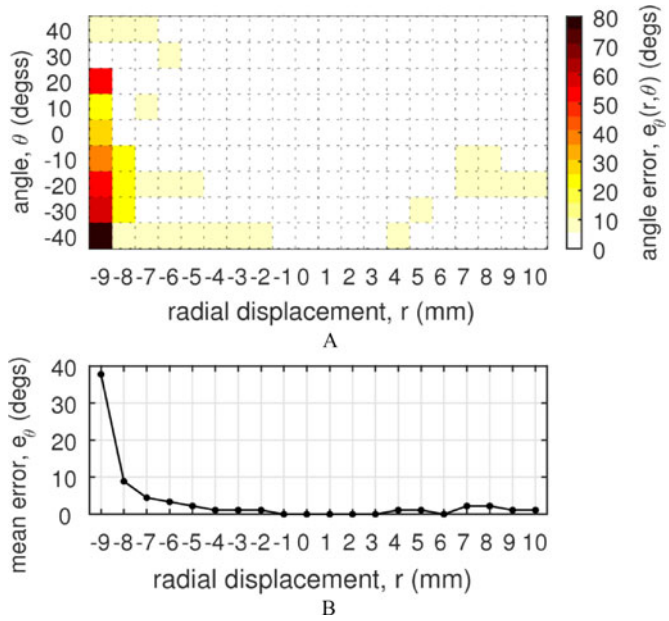

Fig. 6. Angle perception errors for decision after a single contact. (A) Mean angle errors $\bar{e}_\theta(r,\theta)$ evaluated over runs with ground truth (r,θ). (B) Mean errors over all angles in range, depending only on the radial displacement. The best location for perception is in the center of the range $r = 0$ mm. (A) Identity (angle) error. (B) Mean identity (angle) error.

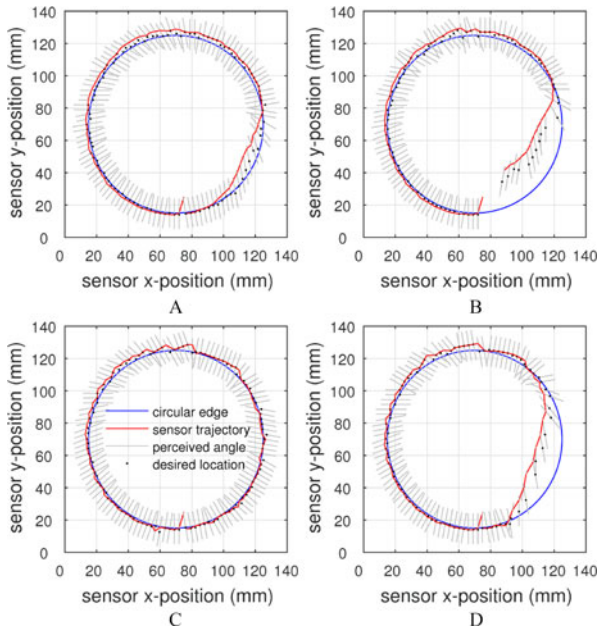

Fig. 7. Exploratory tactile servoing around a circular disk of diameter 110 mm (blue curve). The four panels show the trajectories (red curves) for different radial and angular gains g_r and g_θ in the control policy. Grey lines represent the sensor angle and the location range. Only the combination $(g_r, g_\theta) = (1, 0.5)$ gave successful task completion (panel C). (A) Circular disk ($g_r = 0.5, g_\theta = 0.5$). (B) Circular disk ($g_r = 0.5, g_\theta = 1$). (C) Circular disk ($g_r = 1, g_\theta = 0.5$). (D) Circular disk ($g_r = 1, g_\theta = 1$).

The mean perceptual errors $\bar{e}_\theta(r)$ for edge angle vary smoothly over the radial location range (Fig. 6) from a maximum of $\sim 40^\circ$ at -9 mm away from the edge (with no contact on the object) down to a minimum of zero error in the central region near 0 mm, and then rising again as the sensor moves more fully onto the object. Therefore, actively controlling the sensor to contact the edge in the middle of this location range will lead to the best edge angle decision for the exploratory tactile servoing task.

B. Exploratory Tactile Servoing Around a Circular Disc

Next, we consider the exploratory tactile servoing task (Section III-C) for a circular disc of diameter 110 mm. The task is successfully performed if the tactile robotic system can make a full 360° circuit of the disc's perimeter.

Training data was taken at the bottom position (6 o'clock) on the disk, sampling an edge over 20 radial locations from -9 mm to +10 mm and 9 angles with range -40° to $+40^\circ$ relative to the edge. This data was also used to test biomimetic perception (Section IV-A), validating that $r_{\rm fix} = 0$ mm is a suitable fixation point for active perception.

The exploration task was started at the central training position, at the fixation point $(r_{\rm fix}, \theta_{\rm fix}) = (0\,{\rm mm}, 0^\circ)$. The task was set to explore in a clockwise direction around the disk, with exploration step 3 mm tangential to the perceived edge angle. The decision threshold was set to $E_{\rm dec} = \log 2/N_\theta$, giving angle decisions after 1–3 tactile contacts.

Biomimetic active touch generally gave good task performance, following at least 2/3 of the circumference of the disk in all considered situations (Fig. 7). As the tactile robot traced the edge, it rotated the sensor to maintain its original orientation with the edge (grey normal lines). We attribute the failure in some cases after 2/3 of a cycle (about 2 o'clock) as due to the sensor mis-perceiving edge angle, and then becoming 'lost'. The most likely cause of this failure was from small (sub-millimetre) variations in disk height relative to the robot, so that the test data drifts away from the training data during the task. We examined correcting for this (with some success), but the tuning was both*ad hoc* and laborious. Hence, instead, we consider a more natural (and demanding) test of system performance is to leave these imperfections in the experiment, and instead examine system robustness with respect to task parameters such as the control gains.

Task performance was dependent on the gains g_r and g_θ in the biomimetic active perception algorithm, which control the proportion to move from the estimated radial displacement and angle towards their fixation points. Decreasing the angular gain g_θ from 1 to 0.5 improved task performance (Figs. 7(B), (D) *vs* Figs. 7(A), (B)), presumably because 'bad' sensor rotations are easier to correct. Meanwhile, although decreasing the location gain g_r from 1 to 0.5 resulted in a smoother trajectory (Fig. 7(A) it did not correct large errors. These observations are supported from the RMS tracking errors for Fig. 7(A–D): 1.1 mm, 2.3 mm, 1.0 mm and 0.7 mm. Therefore, the gains $(g_r, g_\theta) = (1, 0.5)$ led to the most robust and accurate performance with successful task completion around the entire edge of the disk (Fig. 7(C)).

C. Application to a Non-Uniform Laminar

To probe the robustness of tactile exploration, we then considered following the edge of a volute (spiral) laminar, where the radius of curvature varies from 20 mm to 50 mm in steps of 10 mm over each half-turn. We consider the volute as

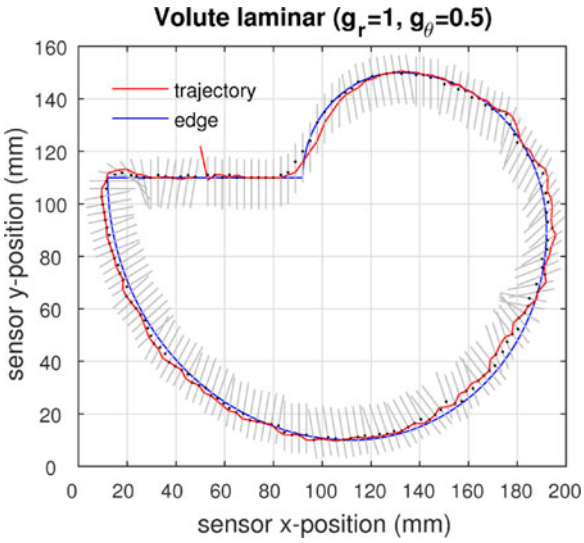

Fig. 8. Exploratory tactile servoing. Other details as in Fig. 7.

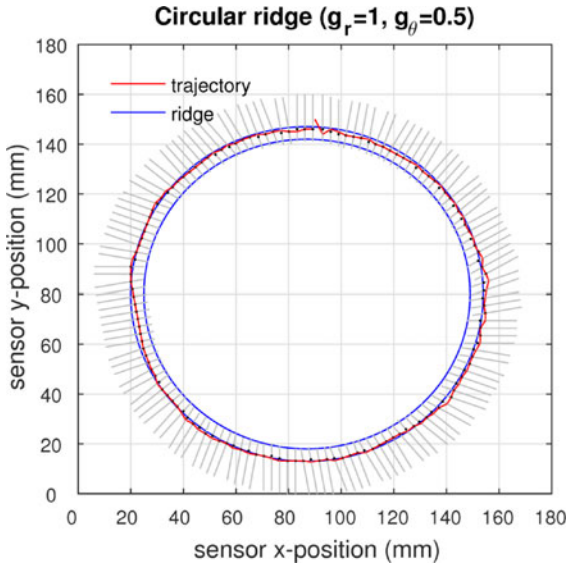

Fig. 9. Exploratory tactile servoing around a circular ridge.

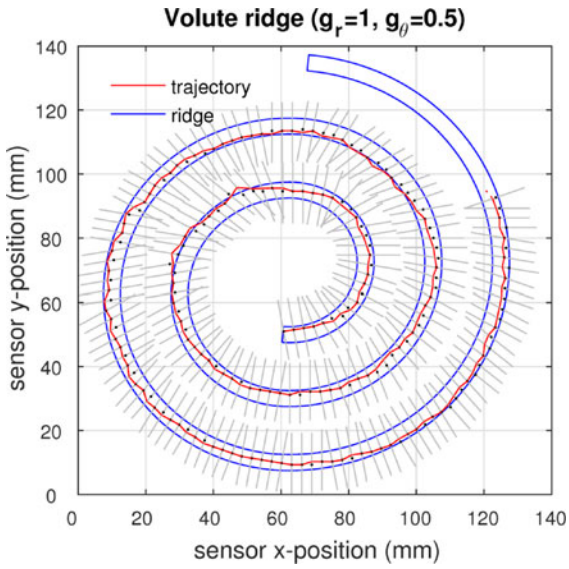

Fig. 10. Exploratory tactile servoing around a volute ridge.

representative of any non-uniform shape with radii of curvature in this range. The task is successfully performed on exploring a full 360° circuit of the perimeter.

Successful task performance was attained (Fig. 8; tracking error 1.2 mm). This performance was with keeping gains $(g_r, g_\theta) = (1, 0.5)$ that were tuned for the disk (Section IV-B). The natural place to train was on the straight edge (near $(50, 110)$ mm on Fig. 8). No other tuning was needed, and the performance worked robustly the first time we set up the experiment, with multiple later runs maintaining similar performance, following a slightly different path each run.

Fundamentally, this test probes the robustness of the perception and exploration method to edge features that differ locally in shape from the original training data. Some generalization capabilities have already been probed with the circular disk, because the contact locations and angles did not lie at the discrete points of the training data (at 1 mm and 10° intervals; Fig. 4). Now also generalization over local edge curvature has been probed. Task performance was best over the bottom 40 mm and 50 mm segments, with both angle and radial location perceived well; angle perception suffered over the top 20 mm and 30 mm segments, but localization was good enough to maintain contact with the edge throughout.

D. Application to Ridges

Finally, we demonstrate that the methods apply more generally than following just the edge of an object, by examining tactile exploration along raised ridges of 5 mm width. In all other respects, the algorithms were identical to those used on edges, apart from that the training data was now collected over the ridge (with the same 20 mm range).

Tactile exploration worked robustly on a circular ridge (Fig. 9) over repeated runs of the experiment. A subtlety is that there is ambiguity (perceptual aliasing) over a 180° rotation of the ridge, which can cause the sensor to flip exploration direction if it drifts too far inwards. We resolved this issue by training the sensor over a more outwards range of the ridge; also the tactile servoing helped because only 90° of training data is needed, which excludes the opposite (180°-rotated) class from the angle perception.

A more demanding task was to follow a volute (spiral) ridge, which the tactile exploration algorithm was able to complete over 810° of rotation (Fig. 10). A major challenge was that the turns of the spiral were only 15 mm apart, to be followed by a tactile sensor with 40 mm dia. hemispherical tip. While it was straightforward to attain robust ridge following over a $\sim$360° turn, if the sensor then drifted a few millimetres from the ridge it would contact and then switch to a neighbouring turn. However, with careful tuning of the training range, the tactile exploration was able to complete this task.

V. Discussion

In this study, we demonstrated robust tactile exploration over various 2D objects, ranging from following the edge of a disk

and volute laminar (of varying curvature), and following along circular and spiral ridges. The methods were adapted from an approach for biomimetic active perception that perceives stimulus identity while controlling sensor location [8]. The method for active touch extends to tactile exploration by modifying the control policy to rotate the sensor to maintain its orientation relative to the edge (tactile servoing) while controlling the radial location (active perception) and moving along a tangential direction (exploration).

This finding helps clarify the relation between haptic exploration [12] and active perception [15], which are distinct leading proposals on the role of action in perception. In robotics and psychophysics, active perception is interpreted as using motor control to aid perception [14], [15], with application to decisions about single tactile features [8]. Likewise, haptic exploration considers 'the hand... uses its motor capabilities to greatly extend its sensory functions' [12], but relates to more complex exploratory procedures such as contour following for feeling shape or enclosure for volume. However, to perform these exploratory procedures, there would need to be ongoing perceptual decisions during the task, suggesting that active perception is a component of haptic exploration [7]. This interpretation motivated past robotics work in which an active perception loop was embedded within an exploration loop [2], [3], [13]. The present study leads to another interpretation: active perception and haptic exploration are distinct instantiations of active touch that differ only in their control policy.

Here we applied a common approach for biomimetic active touch [8] to both a tactile feature (edge angle, Section IV-A) and to haptic exploration around an object (outside edge, Section IV-B, C; ridge, Section IV-D). Task success was assessed by whether the robot could make a complete circuit of the object. The methods worked robustly for edges upon hand-tuning gains in the control policy (Figs. 7, 8), but while successful were not as robust for more demanding objects such as spiral ridges (Fig. 10). In general, we expect that robust exploration will depend upon tuning the control policy to the task, for example with reinforcement learning over task performance.

Our intention with this work is to make progress towards general methods for combining robust control with tactile sensing. By applying methods on biomimetic active perception [8] to exploration, the control aspects of the task performance become more prevalent. For example, we needed to include gains in the control policy, analogous to standard PID feedback control. Our expectation is that progress to more complex tasks of practical interest, such as tactile exploration of three-dimensional objects or continual contact with an object rather than tapping (a challenging problem because of sensor hysteresis), will require more sophisticated control but also benefit from maintaining the biomimetic relation with human and animal perception.

ACKNOWLEDGMENT

The authors would like to thank B. Ward-Cherrier, N. Pestell, and E. Giannaccini for help with this research. The data used in this letter are available for download at http://doi.org/bzrr.

REFERENCES

[1] H. Liu *et al.*, "Finger contact sensing and the application in dexterous hand manipulation," *Auton. Robots*, vol. 39, no. 1, pp. 25–41, 2015.
[2] U. Martinez-Hernandez , T. Dodd, M. Evans, T. Prescott, and N Lepora, "Active sensorimotor control for tactile exploration," *Robot. Auton. Syst.*, vol. 8, no. 7, pp. 7–15, 2017.
[3] U. Martinez-Hernandez, T. Dodd, L. Natale, G. Metta, T. Prescott, and N. Lepora, "Active contour following to explore object shape with robot touch," *World Haptics Conf.*, 2013, pp. 341–346.
[4] Q. Li, C. Schürmann, R. Haschke, and H. Ritter, "A control framework for tactile servoing," in *Proc. Robot., Sci. Syst.*, 2013.
[5] N. Sommer and A. Billard, "Multi-contact haptic exploration and grasping with tactile sensors," *Robot. Auton.. Syst.*, vol. 85, pp. 48–61, 2016.
[6] T. Prescott, M. Diamond, and A. Wing, "Active touch sensing," *Philosoph. Trans. Roy. Soc. B, Biol. Sci.*, vol. 366, no. 1581 pp. 2989–2995, 2011.
[7] N. Lepora, "Active tactile perception," in *Scholarpedia of Touch*. Paris, France: Atlantis Press, 2016, pp. 151–159.
[8] N. Lepora, "Biomimetic active touch with fingertips and whiskers," *IEEE Trans. Haptics*, vol. 9, no. 2, pp. 170–183, Apr. 2016.
[9] N. Lepora, U. Martinez-Hernandez, M. Evans, L. Natale, G. Metta, and T. Prescott, "Tactile superresolution and biomimetic hyperacuity," *IEEE Trans. Robot.*, vol. 31, no. 3, pp. 605–618, Jun. 2015.
[10] N. Lepora and B. Ward-Cherrier , "Superresolution with an optical tactile sensor," in *Proc. IEEE/RSJ Int. Conf. Intell. Robots Syst.*, 2015, pp. 2686–2691.
[11] N. Lepora, U. Martinez-Hernandez, and T. Prescott, "Active touch for robust perception under position uncertainty," in *Proc. IEEE Int. Conf. Robot. Autom.*, 2013, pp. 3005–3010.
[12] S. Lederman and R. Klatzky, "Hand movements: A window into haptic object recognition," *Cogn. Psychol.*, vol. 19, no. 3, pp. 342–368, 1987.
[13] U. Martinez-Hernandez, T. Dodd, T. Prescott, and N. Lepora, "Active Bayesian perception for angle and position discrimination with a biomimetic fingertip," in *Proc. IEEE/RSJ Int. Conf. Intell. Robots Syst.*, 2013, pp. 5968–5973.
[14] J. J. Gibson, *The senses considered as perceptual systems*. Boston, MA, USA: Houghton Mifflin, 1966.
[15] R. Bajcsy, "Active perception," *Proc. IEEE*, vol. 76, no. 8, pp. 966–1005, Aug. 1988.
[16] A. Berger and P. Khosia, "Edge detection for tactile sensing," in *Proc. Robot. Conf.*, 1988, pp. 163–172.
[17] N. Chen, R. Rink, and H. Zhang, "Efficient edge detection from tactile data," in *Proc. IEEE/RSJ Int. Conf. Intell. Robots Syst.*, 1995, pp. 386–391.
[18] T. Phung, Y. Ihn, J. Koo, and H. Choi, "An enhanced edge tracking method using a low resolution tactile sensor," *J. Control, Autom. Syst.*, vol. 8, pp. 462–467, 2010.
[19] T. Assaf, C. Roke, J. Rossiter, T. Pipe, and C. Melhuish, "Seeing by touch: Evaluation of a soft biologically-inspired artificial fingertip in real-time active touch," *Sensors*, vol. 14, no. 2, pp. 2561–2577, 2014.
[20] Z. Su, J. Fishel, T. Yamamoto, and G. Loeb, "Use of tactile feedback to control exploratory movements to characterize object compliance," *Front. Neurorobot.*, vol. 6, no. 7, pp 51–59, 2012.
[21] H. Van Hoof, T. Hermans, G. Neumann, and J. Peters, "Learning robot in-hand manipulation with tactile features," in *Proc. IEEE-RAS 15th Int. Conf. Humanoid Robots*, 2015, pp. 121–127.
[22] J. Fishel and G. Loeb, "Bayesian exploration for intelligent identification of textures," *Front. Neurorobot.*, vol. 6, no. 4, pp. 1–20, 2012.
[23] C. Chorley, C. Melhuish, T. Pipe, and J. Rossiter, "Development of a tactile sensor based on biologically inspired edge encoding," in *Proc. Int. Conf. Adv. Robot.*, 2009, pp. 1–6.
[24] B. Ward-Cherrier, L. Cramphorn, and N. Lepora, "Tactile manipulation with a TacThumb integrated on the open-hand M2 gripper," *IEEE Robot. Autom. Lett.*, vol. 1, no. 1, pp. 169–175, Jan. 2016.
[25] L. Cramphorn, B. Ward-Cherrier, and N. Lepora, "A biomimetic fingerprint improves spatial tactile perception," *IEEE Robot. Autom. Lett.*, 2017, to be published.
[26] N. Lepora, J. Sullivan, B. Mitchinson, M. Pearson, K. Gurney, and T. Prescott, "Brain-inspired bayesian perception for biomimetic robot touch," in *Proc. IEEE Int. Conf. Robot. Autom.*, 2012, pp. 5111–5116.